Authors response to "Contribution of gravity waves to shear in the extratropical lowermost stratosphere: insights from idealized baroclinic life cycle experiments."

Madhuri Umbarkar and Daniel Kunkel
Institute for Atmospheric Physics, Johannes Gutenberg University Mainz, Germany
Correspondence: Madhuri Umbarkar (mumbarka@uni-mainz.de)

We thank the referee for the careful reading and constructive criticism on our manuscript. We understand two major concerns raised by the Reviewer, regarding i) extraction of gravity wave signals, ii) the robustness of the results caused by the model setup, along with some additional scientific clarifications of results interpretations. We hope that our replies to the comments answer the issues in a satisfying way, and that the changes in the manuscript motivated by the comments improved the paper. We first list the central changes in the revised version of the manuscript to give an overview. Then we address each comment in detail and outline the corresponding revisions made to the manuscript (Reviewers comments in italics and corresponding revised text passages are given in italic blue).

Central changes in the revised manuscript

- Motivated by a comment from one of the referees, we have replaced our gravity wave filtering method by incorporating an additional dynamical constraint: the extraction of the divergent wind components using the Helmholtz decomposition technique. In the updated manuscript we derive the small scale effects, i.e., the prime quantities, in the following way:
  1) Extraction of the divergent wind components using the Helmholtz decomposition
  2) Spectral decomposition in which the filter is applied in spectral space using a one-dimensional zonal FFT over the Northern Hemisphere and removes the contributions from wavenumber 0 to 8,
  3) In the subsequent step, we applied an additional Gaussian low-pass filter to the spectral decomposition in the computation of small-scale momentum flux products (i.e., $\overline{u'w'}$ and $\overline{v'w'}$), following the approach of Kruse and Smith (2015).

  This further smoothing better suppresses residual large-scale contributions that may not be fully removed by the initial spectral filtering, thereby improving the separation of small-scale gravity wave effects. This approach affects of prime quantities and thus the figures which show such variables. In detail, we revised Figures 6, 7, 8, 9, 10, 11 and 12 of the original manuscript. We note here that especially the occurrence frequencies of $S^{2'}$ show slightly reduced values but we emphasize that the interpretation of the results and thus the major conclusions drawn from the analysis do not change.

– To address the reviewers concern regarding the realism of moist processes, we included an analysis of 850 hPa relative humidity to show the distribution of the moisture during the baroclinic life cycle. A new appendix figure illustrates its spatial distribution in the MOIST simulations.

– We have added further details on the selection criteria for S^2 and Ri thresholds to clarify the characterization of dynamic instability and shear occurrences across the different experiments.

Response to Reviewer 1

Major comments:

1. Extraction of gravity wave signals

Comment: *I have concerns on the current investigation method for retrieving gravity wave perturbations, in which 8 is chosen as the cutoff wavenumber (either along each latitudinal band by the 1D FFT filter, or over the entire globe by the spherical harmonic filter. For example, as pointed out and exemplified recently by Wei et al. (2022), only using the statistical approach is sometimes not enough when calculating momentum fluxes induced by gravity waves, and it would be better in this case to also include a dynamical approach (e.g., extracting the divergent components of the winds by the Helmholtz decomposition technique). The main reason here is that the scale separation assumption between gravity wave and other signals (e.g., Rossby waves) may not be valid. In particular for this paper, the cutoff wavenumber (if it is referred to as zonal wavenumber 8) is quite small compared with many other studies (e.g., cutoff zonal wavenumber 20 is used in Gupta et al. 2021), and it is possible that Rossby waves are not fully filtered out. One solution here is to apply an additional dynamical constraint (such as the one used in Wei et al. 2022), also with studying the sensitivity of fluxes/Ri to different choices of the cutoff wavenumber by changing it from 8 to 20. I hope that this concern could be addressed or at least discussed in the revision, and the related literature should be mentioned.*

Reply to comment: We agree that combining statistical and dynamical methods can be beneficial, as highlighted in Wei et al. (2022), particularly when the scale separation between gravity waves and Rossby waves is not clear-cut. To address this and to better focus on unbalanced GW dynamics, we now implemented the additional dynamical approach where the divergent components of the winds are extracted by the Helmholtz decomposition technique before the spectral filtering is applied. To further improve the isolation of small-scale gravity wave contributions, we applied a Gaussian low-pass filter during the spectral decomposition step used to compute the momentum flux products (i.e., $\overline{u'w'}$ and $\overline{v'w'}$), followed by Kruse and Smith (2015). This additional smoothing suppresses residual large-scale signals not fully removed by the initial spectral filtering.
Furthermore, to ensure a consistent and physically meaningful calculation of both GWMF and $S^{2'}$, we compute vertical shear from the same spectrally filtered wind components ($u^{'}$, $v^{'}$) which retain the gravity wave signal while yielding smoother and more reliable vertical gradients. Thus, GWMF and $S^{2'}$ pair plots based on the Helmholtz-decomposed wind fields revealed similar behavior as of statistical approach but with shear perturbations maxima being smaller than those of total shear field (see

Figure 3).

Regarding the choice of cutoff, we also conducted a sensitivity test using zonal wavenumber thresholds of 8, 12, and 20. In our idealized setup, we found no significant variation in the resulting GWMF or $S^{2'}$ distributions across these choices: all showed qualitatively and quantitatively similar behavior (see Figure 3). Note that this sensitivity is not a general feature but rather a result of the idealized setup. Based on this, we retained the cutoff at wavenumber 8 for consistency in the remainder of the analysis. We have briefly clarified this and revised Figure 6 to 12 in the manuscript accordingly.

L352: In order to quantify the GW perturbations from synoptic-scale structures, we used a hybrid approach that combines both dynamical and statistical approach to separate large and small scale components of the flow. To better focus on unbalanced GW dynamics, we first follow a dynamical approach in which we separate the wind components into divergent (e.g. u_{div}) and rotational components of the wind using Helmholtz decomposition technique (Wei et al., 2022). We then apply a filter in spectral space to obtain only those contributions from a certain wavenumber onward. In this so-called statistical approach, we use a one-dimensional zonal FFT over the Northern Hemisphere and remove the contributions from wavenumber 0 to 8, e.g., u' is defined as $u' = u_{div} - (u_{div})_{k \leq k_s}$, where k_s being the wavenumber cutoff that splits the quantity into a large scale and small scale components. In our idealized setup, sensitivity tests with k_s values of 12 or 20 showed no significant variation in the resulting GWMF or $S^{2'}$ distributions, indicating that our results are robust with respect to the choice of cutoff. Close to the poles the filtering may remove GW signals as well, but we do not discuss gravity wave contribution in those regions. We emphasize that our spectral definition of the background, along with the dynamical separation into balanced and unbalanced flow, is well justified in the lower stratosphere and consistent with prior studies (Stephan et al., 2019; Gupta et al., 2021; Wei et al., 2022), despite different cutoff wavenumber used.

2. The robustness of the results caused by the model setup

Comment: *As also mentioned in section 6 of the manuscript, 'key processes such as convection were neglected and the representation of GW spectrum may be insufficient to fully capture the complexity of small-scale GW dynamics.' For this reason, I have concerns on the robustness of the results caused by the model setup, especially with a relatively coarse horizontal grid spacing for explicit convection (no convective parameterization is employed). According to Table 1, 20 km is the finest resolution available in this work, which is coarse for explicit convection. Given the important role of latent heating in GW generation, GW amplification and background baroclinic wave life cycles in these simulations, it is important that the authors make a stronger effort to show that their results are robust, and not due to excessive grid-scale latent heating. This could be achieved by (1) performing one simulation with a convective parameterization, and/or (2) performing a convergence test with double horizontal resolution.*

Reply to comment: The aim of our study is to investigate gravity waves in the extratropical lowermost stratosphere associated with baroclinic life cycles, with a specific focus on GWs generated by jet-front systems. To isolate these processes, we focus first on dry dynamics and the gravity waves emerging in this case. Additionally, we put the results from the dry dynamics

into perspective to results from model simulations with minor changes, i.e., inclusion of moisture to include latent heating and inclusion of turbulence. Cloud related parameterizations are discussed to make clear that the latent heating is the important process here. This setup allows us to highlight the importance of latent heating while avoiding additional GW sources from deep convection. Our intention is to clearly address jet/front generated GWs that emerge during baroclinic wave evolution, not the convectively generated GWs.
We agree that GWs from convective sources are important, but addressing them would require full representation of clouds, radiation, and turbulence, which is hardly achievable and thus far beyond the complexity of our current model setup. See also our response to reviewer 2, comment 2.

L125: Note that this study specifically focuses on gravity waves generated by jet–front systems during baroclinic wave evolution. Gravity waves from other sources, such as orography and convection, are not considered, as their adequate representation would require different model configuration and substantially higher resolution which are beyond the scope of this study.

We also sincerely apologize for the error in Table 1. The HRES simulation corresponds to a horizontal grid spacing of $\approx$ 13 km, not 20 km as previously stated. While this resolution is still to coarse to capture resolved convection, it is sufficient to capture the dominant features of baroclinic development and associated gravity wave activity. We have revised Section 2.3.2 to clarify these points and corrected the oversights in Table 1.

3. Additional clarification

3a. Shear versus small-scale shear versus large-scale shear

Comment: *In the current manuscript, the word 'shear' is often used for both small-scale shear and large-scale shear in the text, although their corresponding mathematical expressions are separated from each other. I think that it should be clarified in the text, otherwise it is quite confusing to the readers.*

Also, the authors should also discuss the differences between the generation of the small-scale shear and the generation of the large-scale shear. For example, as far as I am concerned, the large-scale shear can be caused by the baroclinic instability, which is stronger in the moist environment. Also, the breaking gravity waves could also result in the large-scale background wind deceleration/acceleration. Finally, the large-amplitude gravity waves could directly lead to small-scale wind shear, which is generally the case in the current study (if not entirely the case, to the best of my understanding). It is amazing to find low Ri values over the extratropical lowermost stratosphere in such idealized simulations, mainly due to the above small-scale wind shear directly induced by large-amplitude small-scale waves (presumably gravity waves in authors' opinions). However, the below two major questions should be discussed/answered.

Question 1: Which mechanism is responsible for those large-amplitude gravity waves? Are they convectively generated gravity waves? Or, are they similar to jet-front gravity waves in dry environment but largely amplified by the moist processes?

Question 2: Why is the small-scale wind shear so strong over the lowermost stratosphere?

Assuming that the small-scale perturbations are gravity waves, one naive explanation (if not the only) could be provided based on the wavenumber vector refraction equations in the gravity wave linear theory, which include the background wind term (associated with gradients of background wind) and the thermodynamics term (associated with gradients of buoyancy frequency and density scale height). When crossing the tropopause, the thermodynamics term (especially vertical gradients of buoyancy frequency) could be so large that it becomes dominant and tends to shorten gravity wave vertical wavelength, as the case shown in Wei and Zhang (2015; section 5). Therefore, according to the definition in line 356 of the manuscript, the local vertical wind shear could be enhanced due to the dramatic decrease in vertical wavelength associated with the perturbations induced by gravity waves.

Reply to comment: In the revised manuscript, we now consistently refer total shear field to "shear" (S^2) and shear perturbations to "small-scale shear" ($S^{2'}$) wherever appropriate. We have also clarified that the term "enhanced shear" specifically refers to enhancement in the total shear field.

We now explicitly distinguish between large-scale and small-scale shear generation in the revised manuscript Section 4.1.

To answer the first question, in our idealized simulations, the large-amplitude gravity waves observed in the UTLS are primarily generated by imbalances associated with the jet–front system during baroclinic life cycle. This behavior is consistent with previously described jet-front driven gravity wave emission in dry baroclinic life cycles (e.g. Plougonven and Snyder, 2007). We also want to make clear that convection does not play a role in our setup. However, we agree that in moist setups, latent heating can accelerate baroclinic development and thereby amplify the imbalances that lead to gravity wave emission. Although we do not analyze latent heating explicitly in this study, we acknowledge that it can act as a secondary driver of wave generation by modifying the large-scale flow.

Regarding question 2, the strong signs of small-scale wind shear $S^{2'}$ observed in the lowermost stratosphere is due to the presence of gravity waves with short vertical wavelengths. As these waves propagate into the strongly stratified lower stratosphere, the increasing vertical gradient in buoyancy frequency leads to shortening the vertical wavelength of gravity waves. This results in enhanced vertical gradients of the horizontal wind perturbations and thus increases small-scale shear.

This points has been clarified in the section 4.1 of the revised manuscript.

L376: In our baroclinic life cycle setup, vertical shear arises from two main sources: the evolving jet structure and gravity waves. The vertical wind shear is primarily associated with the baroclinic jet, while small-scale vertical shear is mainly induced by large-amplitude gravity waves generated due to imbalances associated with jet-front system during baroclinic wave development. With our setup, we omit GWs from convection and from flow over topography; thus, the emerging GWs are a result of the baroclinic jet–front systems (e.g. Plougonven and Snyder, 2007).

L410: To better understand the physical mechanism behind GWs contribution, we consider the vertical propagation behavior of gravity waves in a strongly stratified environment. The enhanced shear in the lowermost stratosphere is plausibly linked *to the presence of upward-propagating gravity waves. As these waves cross the tropopause, the strong vertical gradient in buoyancy frequency could lead to a shortening the vertical wavelength of gravity waves. This, in turn, increases the vertical gradients of horizontal wind perturbations and thereby enhances local vertical wind shear. This interpretation is consistent with the theoretical framework described in Wei and Zhang (2015).*

3b. Low Ri caused mainly by the small-scale shear versus low Ri caused by both the small-scale shear and large-scale shear versus low Ri caused by local shear and weak N both induced by gravity waves

Comment: *Following the above-mentioned point, low Ri could be caused by either the large-scale vertical wind shear or the small-scale vertical wind shear. However, according to the definition of Ri in line 380, full shear is used for the computation of Ri. It should be clarified which scale of the vertical wind shear contributes more to the formation low Ri.*

In addition to local vertical wind shear, it is also possible that local N (or local potential temperature field) can be influenced by gravity waves. Please verify whether the formation of low Ri depends on the computation of N at different scales.

Reply to comment: In our study, Ri is computed using the total vertical wind shear, which includes both large and small-scale contributions, through the imbalances associated with jet-front system during baroclinic wave development. Our analysis with additional dynamical approach shows significant decrease in the small scale shear occurrences, but their magnitudes are nearly identical. Consequently, the enhanced small scale shear values contribute to low Ri values.

The evolution of N^2 represented in Figure 7a (of original manuscript) and Figure 8a–d of Section 4.1 of the manuscript have shown that N^2 remains relatively consistent between value 2-4 $\times\ 10^{-4} s^{-2}$ with increasing GW activity in the LMS. Meanwhile the vertical shear both S^2 and $S^{2'}$ increases substantially over the several order of magnitudes in the vicinity of GWs. Thus N^2 variability occurs over a much smaller range compared to the vertical shear. This highlights that the low Ri values primarily arise from shear enhancements rather than effects of N^2 at different scales. This has been clarified in the manuscript.

L465: Altogether, the occurrence of low Ri is primarily driven by shear induced by large-amplitude gravity waves, as evidenced by localized regions of strong small scale wind shear despite moderate background shear. This is further supported by the similarity in the distributions of S^2 and $S^{2'}$ in the LMS, particularly in the upper tail of the PDFs shown in Figure 8b–e and 8c–f.

3c. Small-scale processes versus gravity wave processes

Comment: *As mentioned earlier, the scale separation assumption between gravity waves and Rossby waves may not be valid over the upper troposphere and lower stratosphere (UTLS) region in midlatitudes. In order to verify this assumption, a commonly used method can be realized based on a decomposition of kinetic energy into divergent and rotational components. Please compare the energy spectra across different scales between divergent flow and rotational flow, especially over the small scale defined in the current study. I have concerns that only using the statistical approach is not enough over the interested region, and that it is necessary to also include a dynamical approach (e.g., extracting the divergent components of the winds by the Helmholtz decomposition technique).*

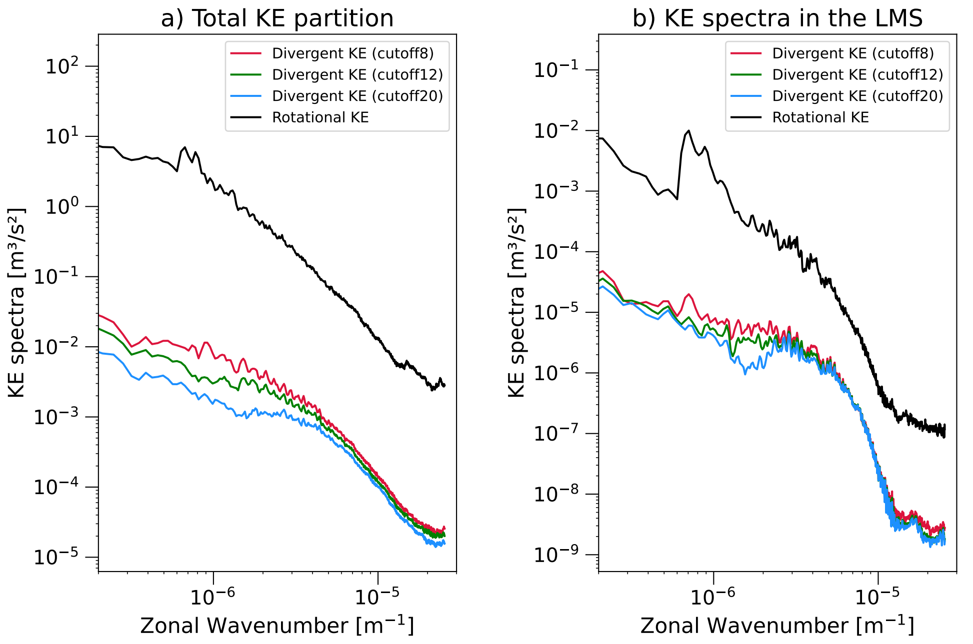

Figure 1. Helmholtz decomposition of wave kinetic energy spectra into rotational and divergent components in the REF simulation. a) Spectra computed for the full domain for different wavenumber cutoffs; b) corresponding spectra restricted to the lowermost stratosphere (LMS).

Reply to comment: Following reviewer comment, we here try to achieve this including additional dynamical constraint. See response to comment 1 for more details. Furthermore, the kinetic energy spectra (Figure 1) of the rotational component follows a k^{-3} slope, characteristic of quasi-geostrophic dynamics, whereas the divergent KE across different wavenumber cutoff exhibits a shallower $k^{-5/3}$ slope, indicative of inertial-range turbulence and small-scale gravity wave activity. In the LMS, at mesoscale and smaller scales, the divergent KE becomes dominant, indicating the increasing influence of unbalanced motions such as gravity waves in the lowermost stratosphere.

3d. Gravity waves versus Rossby waves

Comment: *In order to improve the readability of the paper, please search the word 'wave' over the entire manuscript, and clarify the type of each 'wave' mentioned in the text (e.g., replace it by 'gravity wave' or 'baroclinic/Rossby wave').*

Reply to comment: The text has been revised by specifying "gravity wave" or "Rossby/baroclinic wave" where appropriate to improve clarity and readability.

3e. The realism of the moist processes

Comment: *In order to understand whether the moist processes are realistic in the idealized simulations, please provide more information on the associated meteorological quantities, such as the 1-h precipitation accumulation, the convective available potential energy, and the latent heating rate.*

Reply to comment: While CAPE and precipitation rates are standard in moist convection studies, convection is not central to our objectives and requires a more detailed treatment beyond our idealized setup. Given the role of latent heating in gravity wave generation, we analyze relative humidity (RH) at 850 hPa as a physically consistent quasi-proxy for latent heat release. While RH does not directly measure latent heating, it reflects the distribution of moisture, or more precisely saturation and thus serves as a proxy for the distribution of clouds and moist ascent. A new figure has been added to the appendix B, illustrating the RH distribution in the MOIST simulations.

3f. The threshold/critical values for Ri, S, and any other quantity shown in the entire manuscript

Comment: *The threshold value for the identification of low Ri with potential turbulence is much larger than the theoretical value (e.g., 5 versus 0.25). It is argued by the authors that a larger value is required for the resolution used in the current study. Please clarify exactly how the threshold value of low Ri is related to the resolution, as well as whether the results are sensitive to different threshold values. Otherwise, it will appear to readers that this value is randomly selected or tuned for the optimal results.*

Threshold values for S are also different between dry experiments and other experiments incorporating physical processes, as mentioned in the manuscript. Additional clarification is necessary. Also, the above selected values are much lower than other studies based on ERA5. It is hard to understand why it is the case, as ERA5 is likely coarser than the 20-km simulations in the current study.

In sum, all the threshold/critical values, including Ri, S, and any other quantity if not covered here, should be justified in the manuscript.

Reply to comment: We clarify that in our analysis, regions with Ri ≤ 1 are used to identify dynamically unstable layers, while Ri ≤ 5 highlights regions with **potential for turbulence**. This broader threshold accounts for resolution limitations as coarser grids (from 13 to 80 km) tend to underrepresent sharp shear gradients, resulting in very low Ri values (e.g., $\sim$1 or 0.25) rare in the lower stratosphere (see Kaluza et al., 2022). Additionally in our dry dynamical setup, the forcing of strong shear is generally weaker, which further reduces the occurrence of low Ri values.

Concerning the second part of your comment, we clarify the rationale behind the threshold values for S^2 used in our study. The selection of $S^2 \geq S_t^2$ follows the approach used in Kaluza et al. (2021), where the threshold is based on the criterion that vertical shear exceeding $S^2 \geq S_t^2$ is typically unsustainable under average tropospheric static stability ($\overline{N^2_{trop}}$) leading to low Richardson numbers and increased likelihood of dynamic instability. As shown in their Figure 1 and discussed in their analysis, this criterion links the threshold to physically meaningful limits of shear-induced instability.
In our dry simulations, the mean tropospheric static stability is particularly low, on the order of $0.1 \times 10^{-4} s^{-2}$ due to the

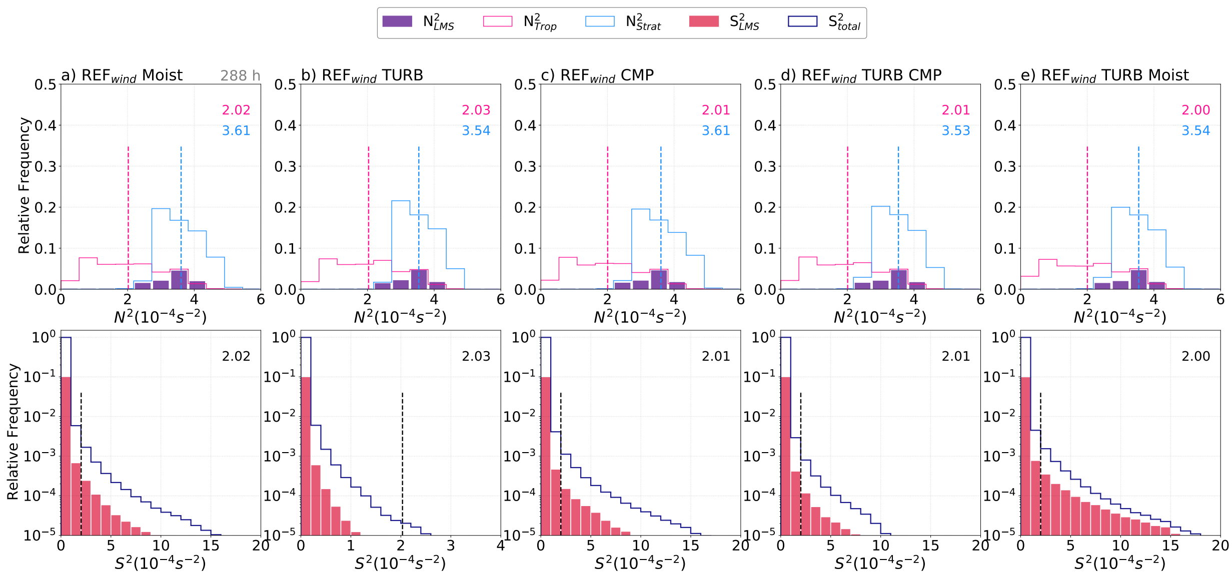

Figure 2. Relative occurrence frequency histogram of static stability and vertical wind shear from 5 km above the surface up to 20 km altitude after 288 h of model integration over the Northern Hemisphere. Counts are weights with grid box volumes: upper panel- static stability. Blue indicates values in the troposphere, pink in the stratosphere and filled purple are of N^2 in the LMS. The corresponding average of tropospheric/stratospheric N^2 are marked with vertical dashed lines. Lower panel- Relative occurrence frequency distribution of vertical wind shear. Purple histograms indicate the S^2 for the selective domain and red filled indicate S^2 in the LMS. Logarithmic occurrence frequency scale. Dash black line indicates threshold value of S^2 for physics sensitivity experiments.

prescribed temperature profile of the idealized setup. This supports the use of a lower threshold value for S^2. Besides this, we have repeated the analysis concerning the vertical distribution of grid volumes in different coordinates for a larger threshold value $1 \times 10^{-4} s^{-2}$. In this analysis, we see that there is a quantitative but no qualitative difference in the shear occurrence frequencies. Moreover, to ensure sensitivity to a full spectrum of shear magnitudes under these low-stability conditions, from the performed threshold sensitivity tests, we found that a threshold of $0.3 \times 10^{-4} s^{-2}$ provides an effective compromise between capturing dynamically relevant shear and enabling consistent comparison across resolutions. For the moist along with other experiments incorporating physical processes, threshold is $2 \times 10^{-4} s^{-2}$ following Kaluza et al. (2021), which reflects the stronger and more frequent shear associated with diabatically enhanced baroclinic development. This choice is supported by the shear and static stability distributions shown in Figure 2, which illustrates the relationship between resolved shear for a representative time step.

Although our threshold values are lower than those used in ERA5-based studies, it is important to note that the overall vertical wind variability due to gravity waves is still underestimated in ERA5, which, if considered for small-scale dynamics, may lead to an underestimation of associated shear. Furthermore, vertical wind shear has been shown to be considerably underestimated at almost all altitudes and across climate zones in ERA5 (Shao et al., 2023). In addition, Schäfler et al. (2020) found that ERA5 significantly underestimates vertical wind shear near the tropopause, especially above upper-tropospheric ridges, key regions critical for the formation of strong shear layers in the extratropics. These limitations are particularly relevant when studying gravity wave–shear interactions using ERA5.

We have clarified this in section 4.2 and section 5 of the revised manuscript accordingly.

L420: We adopt a threshold of Ri ≤ 5 to identify regions with enhanced potential for turbulence, considering previous studies (e.g., Lane et al., 2003; Olsen et al., 2013; Wang and Fu, 2021; Kunkel et al., 2019; Kaluza et al., 2021) and accounting for resolution-dependent effects (e.g., Shao et al., 2023). This threshold ensures consistent comparison across different grid spacings from 13 to 80 km, where small Ri values close to 1 are less likely, particularly in the lower stratosphere (Kaluza et al., 2022). The most unstable and/or potential turbulent regions are still captured using a more conservative threshold of Ri ≤ 1.

L491-496: The identification of the tropopause shear layer requires the definition of a threshold value for S^2. We follow the method used by Kaluza et al. (2021) with adaptation to our baroclinic life cycles. In particular, the threshold value is selected based on the criterion that $S^2 \geq S_t^2$ is typically unsustainable under the average tropospheric static stability ($\overline{N_{trop}^2}$), which results in low Ri and conditions favorable for potential turbulence. Following this, and the average tropospheric static stability $\overline{N_{trop}^2} \approx 2 \times 10^{-4} s^{-2}$ for simulations incorporating physical processes, we use a threshold value $S_t^2 = 2 \times 10^{-4} s^{-2}$, consistent with Kaluza et al. (2021), where latent heating enhances GW activity and shear occurrences. In contrast, dry simulations exhibit much lower mean tropospheric static stability value $0.1 \times 10^{-4} s^{-2}$ due to the prescribed temperature profile of the idealized setup. To adequately capture the full range of dynamically relevant shear in these weakly stable conditions, we adopt a lower threshold of $0.3 \times 10^{-4} s^{-2}$. This value is supported by sensitivity tests, which showed that increasing the threshold (e.g., $1 \times 10^{-4} s^{-2}$) significantly reduced the frequency of identified shear occurrences but did not change the overall distribution patterns. Thus, for dry experiments, the chosen threshold accounts for inherently low shear occurrences and ensures the full spectrum of shear is captured. Therefore, our selected thresholds reflect the underlying differences in static stability and shear environments between dry and moist simulations while maintaining consistency with an established physically based criterion. Note, these values are much lower than the threshold defined in Kaluza et al. (2021), which is mainly rooted in the idealized setup compared to a fully comprehensive reanalysis system.

3g. The definition of lowermost stratosphere

Comment: *It appears to me that the lowermost stratosphere corresponds to the layer above the extratropical tropopause and below the tropical tropopause. Please provide addition clarification/justification on this.*

Reply to comment: This has been explained in the manuscript at L63. We expanded this definition in the revised manuscript by:

P03 L63: More so, the ExTL is part of the lowermost stratosphere (LMS), which can broadly be defined as the region between the height of the extratropical and tropical tropopause (Weyland et al., 2025). The LMS corresponds to the so-called "middle world" where isentropic surfaces intersect the tropopause, allowing for quasi-isentropic exchange between the tropical tropo-

sphere and extratropical stratosphere (Holton et al., 1995). The upper boundary of this layer is commonly approximated by the 380 K isentrope, representing the height of the tropical tropopause (e.g., Appenzeller et al., 1996; Olsen et al., 2013; Wang and Fu, 2021). The LMS encompasses the ExTL, which is characterized by changes in chemical tracer gradients and has been supported by trajectory-based studies (e.g., Hoor et al., 2004; Berthet et al., 2007; Hoor et al., 2010).

We adopt a dynamical tropopause definition, where the extratropical tropopause is represented by the 3.5 PVU isosurface and the tropical tropopause is approximated by the 380 K isentropic level. Accordingly, the LMS in our simulations spans the region between these two surfaces. This clarification has been added to the manuscript as in section 4 as:

P18 L390: The lower boundary of LMS is defined here by the 3.5 PVU dynamical tropopause whereas the 380 K isentrope serves as a upper boundary, which corresponds to the height of the tropical lapse rate tropopause (e.g., Holton et al., 1995; Shepherd, 2007).

Response to Minor comments:

We have carefully addressed all listed points and conducted an additional review of the manuscript to correct remaining issues. Relevant references have been revised or added where appropriate. Please see our point-by-point responses below.

Comment: *1. Line 17 in the Supplement: 'upto' -> 'up to'*

Reply to comment: Done!

Comment: *2. In this manuscript (including the Supplement), both 'Moist' and 'MOIST' are used interchangeably. Also, the first name sometimes is misleading in the sentence. Due to this reason, I would suggest that 'MOIST' should be used in the entire manuscript (including the Supplement and the text shown in the figures).*

Reply to comment: We agree and changed the wording consistently to "MOIST"

Comment: *3. Line 28 in the Supplement: What do you mean by "total moisture" here?*

Reply to comment: By "total moisture," we refer to the sum of water vapor and condensed phases (i.e., cloud water and cloud ice). We have clarified this in the Supplement by replacing "total moisture" with "total content of water vapor and condensed phases (cloud water and ice)" to avoid ambiguity.

Comment: *4. The second line in the caption of Figure S1 (as well as all the other parts in the entire manuscript): "northern hemisphere" -> "Northern Hemisphere"*

Reply to comment: Done!

Comment: *5. The second line in the caption of Figure S1 (as well as all the other parts in the entire manuscript): "Logarithmic occurrence frequency color scale." -> "Logarithmic occurrence frequency color scale is applied."*

Reply to comment: Done!

Comment: *6. The Supplement: Figures in the Supplement are not introduced in the manuscript. I think that it is better to include only the figures (as well as their captions) in the Supplement, and the corresponding discussion/introduction should be shown in the manuscript.*

Reply to comment: Done!

Comment: *7. Line 20 in the manuscript: 'jets' -> 'jet imbalances' (Note: the differences between jets and strong wind shear should be briefly clarified here.)*

Reply to comment: Clarified accordingly in the manuscript.

Comment: *8. Line 29 in the manuscript: 'GWs' -> 'GWs,'*

Reply to comment: Done!

Comment: *9. Line 31 in the manuscript: 'temperature gradients' -> 'horizontal temperature gradients' (Notes: the differences between temperature gradients and atmospheric stability should be briefly clarified here.)*

Reply to comment: Done. Changes given in the response to the comment below.

Comment: *10. Line 33 in the manuscript: This first sentence in this line should be improved. In this particular paragraph, it reads awkwardly and repetitively. I think that this information should be moved ahead as the first/second sentence of this paragraph.*

Reply to comment: We agree and modify the text as follows:

L33: The UTLS is an intriguing region for GW studies, serves both as source and sink, ..., horizontal temperature gradients, as well as abrupt changes in atmospheric stability. While horizontal temperature gradients influence the background wind structure and baroclinicity, vertical stability affects wave amplification and dissipation.

Comment: *11. Line 41 in the manuscript: Please quantify the criteria for the TSL based on S^2.*

Reply to comment: The TSL criterion has now been specified in the revised manuscript.

L41: Such interactions can give rise to the tropopause shear layer (TSL, Kaluza et al., 2021), defined as the region near the extratropical tropopause characterized by the maximum occurrence frequency of $S^2 \geq S_t^2$, where vertical wind shear is given by $\mathrm{S}^2 = \left(\frac{\partial \mathrm{u}}{\partial \mathrm{z}}\right)^2 + \left(\frac{\partial \mathrm{v}}{\partial \mathrm{z}}\right)^2$, i.e. the squared vertical gradient of the horizontal wind components u and v. Following Kaluza et al. (2021), regions of enhanced shear are defined as those where S^2 exceeds a threshold value S_t^2, which corresponds to the 95^{th}

percentile of total S^2 values within a climatological dataset. This statistical approach allows the identification of particularly strong shear events associated with tropopause disturbances.

Comment: *12. Line 64 in the manuscript: This definition is confusing to me. Why is tropical tropopause relevant over midlatitudes?*

Reply to comment: The definition has been clarified in our response to Comment 3g, we have revised this part of the manuscript to clarify the definition.

Comment: *13. Line 87 in the manuscript: 'are' -> 'which are'*

Reply to comment: Done!

Comment: *14. Line 149 in the manuscript: I believe that 'TKE' is shown for the first time here in this draft, and the full name should be given, if this is the case. Also, a full name of 'TKE' is somehow provided in line 408 in the manuscript. Please consider providing this information (as well as all the other short names) as early as possible, in order to improve the readability.*

Reply to comment: We have now introduced the full term "turbulent kinetic energy (TKE)" at its first mention in the manuscript.

Comment: *15. Line 186 in the manuscript: What do you mean by 'a third initial state'? Please clarify.*

Reply to comment: We have mentioned "a third initial state" refers to a baroclinic wave test case following Jablonowski et al. 2006, which is used alongside the two DCMIP initial states. This has now been removed for better readability.

Comment: *16. Figure 1: Bad contour design. It is hard to tell one field from another. Also, the dynamical tropopause and extratropical tropopause should be the same thing in this manuscript. Please clarify this point (or simply use either one of them throughout the entire manuscript).*

Reply to comment: Regarding the figure, we have adjusted the color scheme. We used the term "extratropical dynamical tropopause" in the manuscript accordingly.

Comment: *17. Line 199 in the manuscript: '13' -> '20' (Note: inconsistency between this line and the table)*

Reply to comment: It is a typo. We have corrected the value based on resolution in the table.

Comment: *18. Lines 228-230 in the manuscript: I am not sure whether these two statements hold true. First, how to quantify whether the GW emission is less or more? Second, how to verify whether the results are more conservative or less conservative? Third, exactly how does fast growth rate of the baroclinic wave result in the so-called numerical, spurious features?*

Reply to comment: Thank you for pointing that out.

1) We do not quantify GW emission explicitly in this section. Instead, we qualitatively associate slower baroclinic wave growth with reduced excitation of gravity waves, based on the idea that more gradual flow evolution may generate fewer transient imbalances.

2) "More conservative" is used here for a more gradual growth.

3) To our understanding, rapid growth can induce sharp gradients and strong imbalances in the model fields, which may enhance numerical noise or non-physical wave generation. Slower evolution helps mitigate these effects, allowing better isolation of physical processes.

Comment: *19. Line 233 in the manuscript: 'wave breaking' -> 'baroclinic wave breaking' (Note: the authors should check the entire manuscript and briefly clarify which type of wave is mentioned.)*

Reply to comment: Noted. The text has been revised by specifying "gravity wave" or "Rossby/baroclinic wave" where appropriate to improve clarity and readability.

Comment: *20. Line 250 in the manuscript: 'Plougonven and Zhang, 2013' -> 'Plougonven and Zhang, 2014' (Note: Please double check the entire manuscript.)*

Reply to comment: Done!

Comment: *21. Lines 254-255 in the manuscript: I am sure whether the work of Wang and Zhang (2007) is cited correctly. In Wang and Zhang (2007), several dry baroclinic wave idealized simulations are performed with varying baroclinic instability, in order to understand the sensitivity of mesoscale gravity waves to the baroclinicity of jet-front systems. Note that this comparison is done at the exact same phase of different baroclinic wave life cycles. However, in this manuscript, it is about the same baroclinic wave life cycle but at different phases.*

Reply to comment: Thank you for pointing that out, it was an oversight.

Comment: *22. Figure 4: It is hard to understand the discussion on this figure, since the wind/pressure field is not shown and it is hard to identify the location of ridge/trough.*

Reply to comment: We have now included 3.5 PVU potential vorticity isosurface to the figure.

Comment: *23. Line 258 in the manuscript: Delete 'sort of'.*

Reply to comment: Done!

Comment: *24. Line 274 in the manuscript: 'wave' -> 'waves'*

Reply to comment: Done!

Comment: *25. Line 274 in the manuscript: 'in the' -> 'in'*

Reply to comment: Done!

Comment: *26. Line 275 in the manuscript: 'occurrence' -> 'occurrences'*

Reply to comment: Done!

Comment: *27. Line 276 in the manuscript: '11-km' -> '11-km altitude'*

Reply to comment: Done!

Comment: *28. Line 296-299 in the manuscript: Please add '(1) . . . , (2) . . . , (3). . . ' after 'including'.*

Reply to comment: Done!

Comment: *29. Line 311 in the manuscript: How to make sure that those synoptic-scale waves are gravity waves (instead of baroclinic waves)?*

Reply to comment: We agree that the term "synoptic-scale gravity waves" may be misleading, as gravity waves typically occur at smaller scales than baroclinic waves. We have revised the sentence using "gravity waves".

Comment: *30. Line 314 in the manuscript: I would suggest that the cited two references should be replaced by Wei and Zhang (2014) and Wei et al. (2016), since I think that the current references are cited incorrectly here. Neither of them is based on the study of simulated idealized moist baroclinic wave life cycles. The first paper cited in this line (i.e., Zhang 2004) is based on the dry simulations, instead of moist simulations. The second paper cited in this line (Zhang et al. 2015b) is mainly based on observations, instead of simulations.*

Reply to comment: That is correct! Cited accordingly.

Comment: *31. The second line in the caption of Figure 6: What are the contour levels for absolute GW momentum flux?*

Reply to comment: The contour levels for absolute gravity wave momentum flux in Figure 6 are set from 1.5 to 3.0 log10(mPa) to highlight higher |GWMF| values observed in the dry simulations ensuring visibility of dynamically active regions.

Comment: *32. Line 334 in the manuscript: What do you mean by 'a vertical gradient barrier'? What is the specific definition here?*

Reply to comment: We agree that the term "vertical gradient barrier" was unclear. Modified "creating a vertical gradient barrier" to "..sharp vertical gradients in stability and moisture"

Comment: *33. Line 351 in the manuscript (as well as all the other parts in the entire manuscript): 'divergence' -> 'horizontal divergence'*

Reply to comment: Done!

Comment: *34. Line 351 in the manuscript: 'both are' -> 'they are'*

Reply to comment: Done!

Comment: *35. Line 352 in the manuscript: 'w' as all other prime quantities here represent filter quantities.' -> 'As all the other prime quantities, w' here represents filtered quantities.'*

Reply to comment: Corrected!

Comment: *36. Lines 353-354 in the manuscript: What filter is used here? Spherical harmonic filter over the entire globe? Or the 1D FFT filter over each zonal direction with the cutoff zonal wavenumber at 8? Please clarify. Also, regardless of the filter method, the cutoff wavenumber appears to be rather low, compared with many published articles.*

Reply to comment: See our response to major comment 1 and 3c.

Comment: *37. The equation in line 354 in the manuscript (as well as all the other parts in the entire manuscript): This equation, listed in a single line, should be numbered.*

Reply to comment: Done!

Comment: *38. The equation in line 354 in the manuscript: It is not clear to me how the overline is computed. This information, as well as all the other procedures in the computation, is important, otherwise it will be hard for others to reproduce the results in the future. As a potential example, please check section 2d in Wei et al. (2022).*

Reply to comment: Thank you for the reference. We were not previously aware of this diagnostic approach and have now clarified it in the revised manuscript.

L355: The overline denotes a spatial average of the perturbation products (i.e. $\overline{u'w'}$ and $\overline{v'w'}$) computed using a low-pass filtering of the quadratic quantities which uses the same Gaussian spectral filter as mentioned in Kruse and Smith (2015). This averaging ensures that the flux estimates are physically meaningful, as direct pointwise computation of these second-order terms without low-pass filtering or areal averaging would not appropriately capture the wave-induced momentum transport (see also Wei et al., 2022). This approach is consistent with the statistical method of scale separation commonly used in gravity wave studies (e.g., Lehmann et al., 2012; Wei et al., 2016).

Comment: *39. Line 359 in the manuscript: I am not sure about the expression of 'divergence-convergence of vertical velocity'. It appears that they are treated as the same. Horizontal divergence and vertical velocity may be related, but they have different mathematical expressions with different units.*

Reply to comment: The wording has been modified accordingly.

L359: "... alternating regions of upward and downward vertical velocity perturbations…"

Comment: *40. Line 385 in the manuscript: 'We also regard' -> 'Following this idea, we regard'*

Reply to comment: Done!

Comment: *41. Lines 389-390 in the manuscript: This is confusing to the readers. Do both the 3.5-PVU level and the 380-K isentropic level correspond to the feature mentioned here? Also, what do you mean by 'the maximum potential temperature of the tropical lapse rate tropopause'?*

Reply to comment: We acknowledge that the phrase "maximum potential temperature of the tropical lapse rate tropopause" was misleading. We have revised the sentence to clarify that the 380 K isentrope is used as a proxy for the tropical tropopause, following the literature.

Comment: *42. Line 401 in the manuscript: Please double check whether the S^2 and $S^{2'}$' is correct here.*

Reply to comment: Yes, it is. Changed to "An analysis of N^2, S^2 and $S^{2'}$ ..." to avoid confusion.

Comment: *43. Figure 9: I don't understand why lines of 'Ri=1' are not shown in Figure 9a (upper and lower subplots).*

Reply to comment: Thank you for the mention. We have now updated the figure accordingly.

Comment: *44. The lower subplots in Figure 9 (as well as all the other parts in the manuscript): Please clarify whether S^2 or $S^{2'}$ is used in the computation of Ri. It appears to me that $S^{2'}$ is used here, which is different from the original definition of Ri.*

Reply to comment: We confirm that the original definition of the Richardson number (Ri) is used in our analysis, where the full vertical shear S^2 (and not the shear perturbations $S^{2'}$), is used in the computation. We have clarified this in the manuscript to avoid confusion.

L380: Note that Ri is computed using the full vertical shear S^2, to initially assess turbulence-prone regions throughout the baroclinic flow.

Comment: *45. Line 423 in the manuscript: 'the the' -> 'the'*

Reply to comment: Done!

Comment: *46. Line 424 in the manuscript: 'between' -> 'among'*

Reply to comment: Done!

Comment: *47. The second line in the caption of Figure 11: What do you mean by 'pairs'?*

Reply to comment: It was a typo. ",pairs"-> "pair" makes it readable to |GWMF|-S2' pair.."

Comment: *48. Line 462 in the manuscript (as well as all the other parts in the entire manuscript): Are the 'the sub-synoptic waves' mentioned in this line gravity waves or Rossby waves?*

Reply to comment: We agree that the original phrasing was ambiguous. Here we refer Rossby waves, associated with large-scale flow features, rather than gravity waves. We have revised the text in the manuscript.

L462: "... related to Rossby waves, as it is linked to large-scale flow features rather than small-scale gravity wave activity."

Comment: *49. Line 462 in the manuscript: I think that there is an error in the printed text for the* $N^{2'}$*, with a redundant prime notation.*

Reply to comment: It was a typo.

Comment: *50. Figure 13a: For each vertical cross section plot, the corresponding line in the horizontal view (as well as the wave signals in the horizontal view) should be given.*

Reply to comment: The corresponding lines have now been added to the horizontal view in Figure 6.

Comment: *51. The last two lines in the caption of Figure 13: 'The zonal mean dynamical tropopause altitude is indicated by the dashed black line and tropical tropopause (380 K isentrope) by grey dashed line.' -> 'The zonal mean value of 3.5 PVU in the potential vorticity field is indicated by the dashed black line, and the zonal mean value of 380 K in the potential temperature field is indicated by the grey dashed line.'*

Reply to comment: Done!

Comment: *52. Line 478 in the manuscript: 'we will now explore in more detail' -> 'we will explore in the next section with more detail'*

Reply to comment: Done!

Comment: *53. Line 481 in the manuscript: 'and the potential' -> ', as well as the potential' (Note: there are two 'and's in the sentence.)*

Reply to comment: Done!

Comment: *54. Line 485 in the manuscript: 'tropopause following coordinate' -> 'the tropopause-following coordinate'*

Reply to comment: Done!

Comment: *55. Line 487 in the manuscript: 'occur' -> 'are'*

Reply to comment: Done!

Comment: *56. Lines 491-492 in the manuscript: It is hard to follow this sentence.*

Reply to comment: We have changed the wording for clarity. See our response to comment 3f.

Comment: *57. Line 493 in the manuscript: I am not sure why threshold values are different between dry runs and other runs incorporating more complex physical processes. I think that it is better to keep them consistent.*

Reply to comment: We agree that the thresholds differ. As previously explained in our response to comment 3f, the selected values reflect the differing static stability and shear environments in dry versus moist simulations, while remaining consistent with the physically based criterion introduced by Kaluza et al. (2021).

Comment: *58. Line 519 in the manuscript: ‘due’ -> ‘by’*

Reply to comment: Done!

Comment: *59. Line 525 in the manuscript: ‘vertical wind shear and potential turbulence and their contribution’ -> ‘vertical wind shear, potential turbulence, and their contribution’*

Reply to comment: Done!

Comment: *60. Line 542 in the manuscript: This is not a new paragraph. Please remove the redundant blank space in the previous line.*

Reply to comment: Done!

Comment: *61. Line 552 in the manuscript: ‘the breaking of synoptic scale wave’ -> ‘the breaking of synoptic scale baroclinic wave’*

Reply to comment: Done!

Comment: *62. Please consider citing the work of Zhang et al. (2015a), which has investigated the UTLS GWs associated with the jet streak observed by the aircraft measurement.*

Reply to comment: Done!

Comment: *63. Please consider citing the work of Plougonven and Snyder (2007), which has compared GW characteristics between different baroclinic life cycles.*

Reply to comment: Done!

Comment: *64. Over the entire manuscript (including the figures): ‘pvu’ -> ‘PVU’*

Reply to comment: Done!

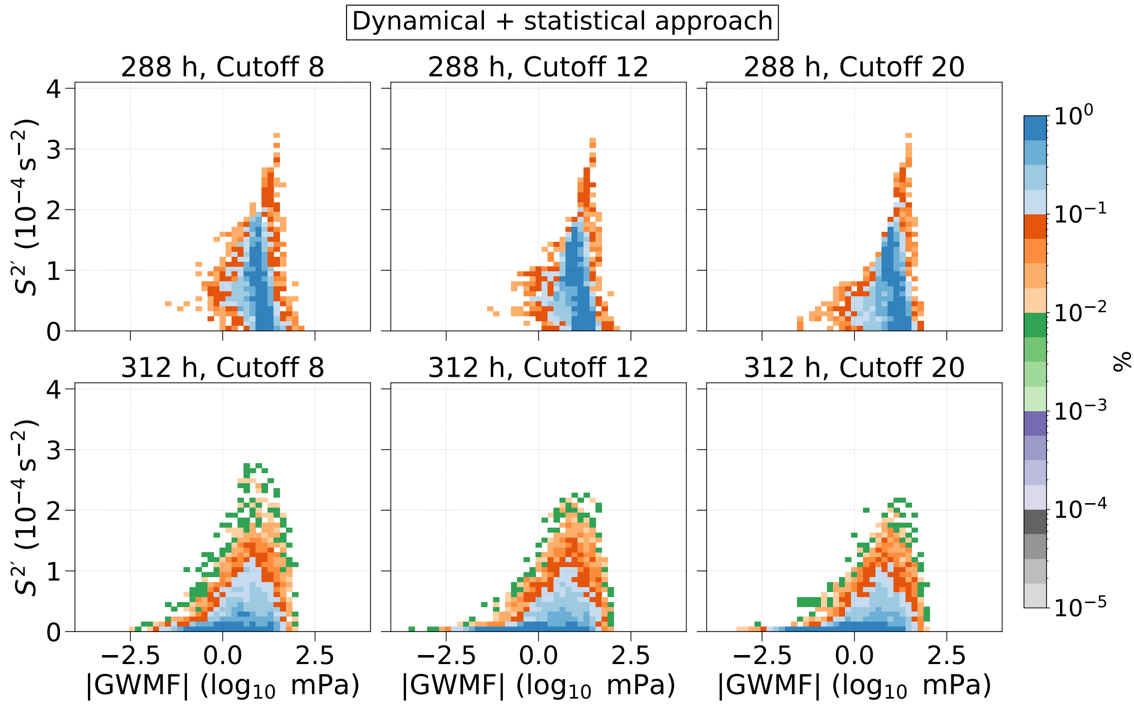

Figure 3. Relative occurrence frequency or probability density distribution of absolute momentum flux due to GWs |GWMF| - vertical shear perturbations $S^{2'}$ pair in the LMS for Ri $\leq$ 5 for simulations with different wavenumber cutoff sensitivity.

References

Appenzeller, C., Holton, J. R., and Rosenlof, K. H.: Seasonal variation of mass transport across the tropopause, Journal of Geophysical Research: Atmospheres, 101, 15 071–15 078, https://doi.org/10.1029/96jd00821, 1996.

Berthet, G., Esler, J. G., and Haynes, P. H.: A Lagrangian perspective of the tropopause and the ventilation of the lowermost stratosphere, Journal of Geophysical Research: Atmospheres, 112, https://doi.org/10.1029/2006jd008295, 2007.

Gupta, A., Birner, T., Dörnbrack, A., and Polichtchouk, I.: Importance of Gravity Wave Forcing for Springtime Southern Polar Vortex Breakdown as Revealed by ERA5, Geophysical Research Letters, 48, https://doi.org/10.1029/2021GL092762, 2021.

Holton, J. R., Haynes, P. H., McIntyre, M. E., Douglass, A. R., Rood, R. B., and Pfister, L.: Stratosphere-troposphere exchange, Reviews of Geophysics, 33, 403–439, https://doi.org/10.1029/95RG02097, 1995.

Hoor, P., Gurk, C., Brunner, D., Hegglin, M. I., Wernli, H., and Fischer, H.: Seasonality and extent of extratropical TST derived from in-situ CO measurements during SPURT, Atmospheric Chemistry and Physics, 4, 1427–1442, https://doi.org/10.5194/acp-4-1427-2004, 2004.

Hoor, P., Wernli, H., Hegglin, M. I., and Bönisch, H.: Transport timescales and tracer properties in the extratropical UTLS, Atmospheric Chemistry and Physics, 10, 7929–7944, https://doi.org/10.5194/acp-10-7929-2010, 2010.

Kaluza, T., Kunkel, D., and Hoor, P.: On the occurrence of strong vertical wind shear in the tropopause region: a 10-year ERA5 northern hemispheric study, Weather and Climate Dynamics, 2, 631–651, https://doi.org/10.5194/wcd-2-631-2021, 2021.

Kaluza, T., Kunkel, D., and Hoor, P.: Analysis of Turbulence Reports and ERA5 Turbulence Diagnostics in a Tropopause-Based Vertical Framework, 49, e2022GL100 036, https://doi.org/10.1029/2022GL100036, 2022.

Kruse, C. G. and Smith, R. B.: Gravity Wave Diagnostics and Characteristics in Mesoscale Fields, Journal of the Atmospheric Sciences, 72, 4372–4392, https://doi.org/10.1175/jas-d-15-0079.1, 2015.

Kunkel, D., Hoor, P., Kaluza, T., Ungermann, J., Kluschat, B., Giez, A., Lachnitt, H. C., Kaufmann, M., and Riese, M.: Evidence of small-scale quasi-isentropic mixing in ridges of extratropical baroclinic waves, Atmospheric Chemistry and Physics, 19, 12 607–12 630, https://doi.org/10.5194/acp-19-12607-2019, 2019.

Lane, T. P., Sharman, R. D., Clark, T. L., and Hsu, H.-M.: An Investigation of Turbulence Generation Mechanisms above Deep Convection, Journal of the Atmospheric Sciences, 60, 1297–1321, https://doi.org/10.1175/1520-0469(2003)60<1297:aiotgm>2.0.co;2, 2003.

Lehmann, C. I., Kim, Y.-H., Preusse, P., Chun, H.-Y., Ern, M., and Kim, S.-Y.: Consistency between Fourier transform and small-volume few-wave decomposition for spectral and spatial variability of gravity waves above a typhoon, Atmospheric Measurement Techniques, 5, 1637–1651, https://doi.org/10.5194/amt-5-1637-2012, 2012.

Olsen, M. A., Douglass, A. R., and Kaplan, T. B.: Variability of extratropical ozone stratosphere–troposphere exchange using microwave limb sounder observations, Journal of Geophysical Research: Atmospheres, 118, 1090–1099, https://doi.org/10.1029/2012jd018465, 2013.

Plougonven, R. and Snyder, C.: Inertia-gravity waves spontaneously generated by jets and fronts. Part I: Different baroclinic life cycles, Journal of the Atmospheric Sciences, 64, 2502–2520, https://doi.org/10.1175/JAS3953.1, 2007.

Shao, J., Zhang, J., Wang, W., Zhang, S., Yu, T., and Dong, W.: Occurrence frequency of subcritical Richardson numbers assessed by global high-resolution radiosonde and ERA5 reanalysis, Atmospheric Chemistry and Physics, 23, 12 589–12 607, https://doi.org/10.5194/acp-23-12589-2023, 2023.

Shepherd, T. G.: Transport in the Middle Atmosphere, Journal of the Meteorological Society of Japan. Ser. II, 85B, 165–191, https://doi.org/10.2151/jmsj.85B.165, 2007.

Stephan, C. C., Strube, C., Klocke, D., Ern, M., Hoffmann, L., Preusse, P., and Schmidt, H.: Intercomparison of Gravity Waves in Global Convection-Permitting Models, Journal of the Atmospheric Sciences, 76, 2739–2759, https://doi.org/10.1175/jas-d-19-0040.1, 2019.

Wang, M. and Fu, Q.: Stratosphere-Troposphere Exchange of Air Masses and Ozone Concentrations Based on Reanalyses and Observations, Journal of Geophysical Research: Atmospheres, 126, https://doi.org/10.1029/2021jd035159, 2021.

Wei, J. and Zhang, F.: Tracking gravity waves in moist baroclinic jet-front systems, Journal of Advances in Modeling Earth Systems, 7, 67–91, https://doi.org/10.1002/2014ms000395, 2015.

Wei, J., Zhang, F., and Richter, J. H.: An Analysis of Gravity Wave Spectral Characteristics in Moist Baroclinic Jet–Front Systems, Journal of the Atmospheric Sciences, 73, 3133–3155, https://doi.org/10.1175/jas-d-15-0316.1, 2016.

Wei, J., Zhang, F., Richter, J. H., Alexander, M. J., and Sun, Y. Q.: Global Distributions of Tropospheric and Stratospheric Gravity Wave Momentum Fluxes Resolved by the 9-km ECMWF Experiments, Journal of the Atmospheric Sciences, 79, 2621–2644, https://doi.org/10.1175/jas-d-21-0173.1, 2022.

Weyland, F., Hoor, P., Kunkel, D., Birner, T., Plöger, F., and Turhal, K.: Long-term changes in the thermodynamic structure of the lowermost stratosphere inferred from reanalysis data, Atmospheric Chemistry and Physics, 25, 1227–1252, https://doi.org/10.5194/acp-25-1227-2025, 2025.